INTERNATIONAL ATOMIC ENERGY AGENCY
UNITED NATIONS EDUCATIONAL, SCIENTIFIC AND CULTURAL ORGANIZATION

INTERNATIONAL CENTRE FOR THEORETICAL PHYSICS
34100 TRIESTE (ITALY) - P.O.B. 586 - MIRAMARE - STRADA COSTIERA 11 - TELEPHONES: 224281/2/3/4/5/6
CABLE: CENTRATOM - TELEX 460392-1

SMR/115 - 28

WINTER COLLEGE ON LASERS, ATOMIC AND MOLECULAR PHYSICS

(21 January - 22 March 1985)

- TUNABLE SOLID STATE LASERS
- DIFFERENCE FREQUENCY GENERATION AND PARAMETRIC GENERATION
- STIMULATED RAMAN SCATTERING

D.C. HANNA
Department of Electronics
The University of Southampton
Southampton SO9 5NH
U.K.

Tunable Solid State Lasers (U.K.)

The discovery of very broad emission bands from ion impurities and the demonstration of widely tunable laser emission dates back to the early days of lasers [1]-[4]. The theory of such lasers was developed by McCumber [5]. The laser materials studied by Johnson and co-workers involved impurities such as Ni^{2+}, Co^{2+} and V^{2+} in host crystals such as MgF_2, MnF_2 and rutile. The essential features of the energy level scheme are shown below. Emission from the upper laser level can terminate at a level above the ground level, corresponding to the excitation of a lattice vibration. Such laser emission has been called 'phonon-terminated'

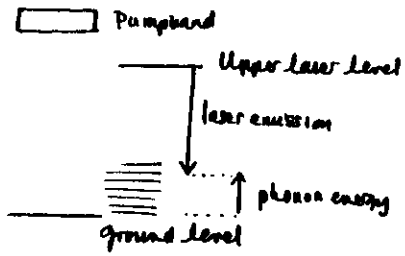

At a low enough temperature (typically operation at ~ 77K is involved) the phonon population is reduced sufficiently for this laser to behave more or less as a four level laser, i.e. the lower laser level is essentially empty. The early work of Johnson was based on the use of flash lamp pumping or continuous pumping with a tungsten lamp. Despite the complication of working at cryogenic temperatures the performance of the $Ni^{2+}:MgF_2$ system was quite impressive, a cw threshold power of 65W with the tungsten lamp being achieved

Interest in these phonon-terminated lasers quickly diminished with the appearance of efficient rare-earth doped lasers such as NdYAG. However, after a period of nearly fifteen years, interest was rekindled by the work of Moulton and Mooradian who applied the idea of laser-pumping to the $Ni^{2+}:MgF_2$ and $Co^{2+}:MgF_2$ lasers [6-9]. A 1.3 μm NdYAG laser has been used as the pump (or $Nd\,YAlO_3$ [9]), either operated cw or pulse pumped. The $Ni^{2+}:MgF_2$ and $Co^{2+}:MgF_2$ lasers have been operated c.w, Q-switched, and mode-locked. Wide tuning range, high power operation, and very efficient operation have all been demonstrated. Some figures below illustrate this. For example $Co^{2+}:MgF_2$ has tuned from 1.6 - 2.2 μm [9], and $Ni^{2+}:MgF_2$ from 1.61 to 1.74 μm. Mode-locked operation of $Co^{2+}:MgF_2$ has yielded pulses as short as 34 psec [8], and $Ni^{2+}:MgF_2$ gave 23 psec. Q-switched operation of $Co^{2+}:MgF_2$ has given 20 mJ TEM_{00} output in ~ 200 nsec pulses, i.e 100 kW peak power. Energy conversion efficiency, from 1.3 μm pump to 1.9 μm output of ~25% has been obtained in $Co^{2+}:MgF_2$, and an average output power of 7 W for a 1.3 μm input of 35 W [9].

As the temperature is raised from liquid N_2 temperature the fluorescence lifetime decreases (1.3 ms at 80 K to 0.3 ms at 225 K). This raises the threshold for cw pumping, however if the pump pulse duration is shorter than the fluorescence lifetime the threshold need not increase. Moulton has demonstrated this using a two-stage Marx selective

cooler, reaching 225 K, and found a threshold at 1.97 μm which was comparable to that obtained at 90 K. Higher temperature operation would undoubtedly increase the applications of the $Co^{2+}:MgF_2$ lasers since the need for cryogenic temperature has been something of a drawback. Another drawback is the fact that the stimulated emission cross section is small, $\sim 1.5 \times 10^{-21}\ cm^2$ peak value. This means that the laser can only have a modest gain and this has a number of consequences. Thus considerable care must be taken to minimise losses in the resonator. Either spaces must be at Brewster's angle or have very low loss anti-reflection coatings. This is particularly important where intracavity elements such as Q-switches, mode-lockers and frequency selectors are used. The small gain also means that a correspondingly large fluence is involved in Q-switched operation and this increases the risk of damage.

Other related laser materials are $Co^{2+}:KZnF_3$ and $Ni^{2+}:KMgF_3$. [10,11] and the search for improved materials continues. The particular feature which would be most desirable is the possibility of room temperature operation. However the example of $Ni^{2+}:KMgF_3$ [11] illustrates the difficulties and disappointments that can be encountered. $Ni^{2+}:KMgF_3$ shows a long fluorescence lifetime and high quantum efficiency at room temperature but it was found that operation above 195 K did not occur. The conjecture is that excited state absorption so reduced the gain that oscillation was prevented. Excited state absorption is difficult to measure and since the laser gain is small a similarly small excited state absorption

may make all the difference between success and failure. The long wavelength limit ($\sim 1.74\,\mu m$) for the cw $Ni^{2+}:MgF_2$ laser is also thought to be imposed by excited state absorption [9] since fluorescence emission occurs to significantly longer wavelengths.

Another class of tunable solid state lasers that has been creating interest in recent years is based on the Cr^{3+} ion as impurity. Ruby is the best known example of a laser based on the Cr^{3+} but it operates as a 3-level laser with the laser transition being a narrow ($\sim 10\,cm^{-1}$) no-phonon line. Different host materials have a significant effect on some of the energy levels of the Cr^{3+} ion. In Alexandrite ($BeAl_2O_4 : Cr^{3+}$) it is found that while the ^2E level is in much the same position as in ruby and gives rise to the same 3-level laser operation, the $^4T_2$ level is much closer to the ^2E level in Alexandrite. The $^4T_2$ population is in thermal equilibrium with the metastable ^2E level and has a sufficient population to allow laser oscillation on the transition $^4T_2 \rightarrow {}^4A_2$ (ground level). This emission is phonon-terminated, and leads to widely tunable 4 level operation, as illustrated below.

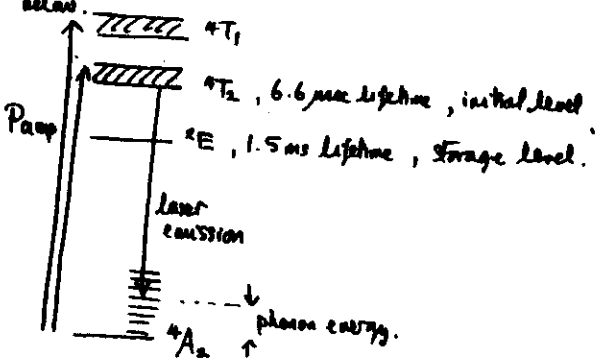

A detailed modelling of the behaviour of the Alexandrite laser, particularly with regard to its temperature dependence, is still the subject of development and investigation. The complicating features are as follows. ① Temperature change affects the phonon population and therefore the population of the terminal level of the laser.
② Temperature change alters the relative population of the storage level and the initial laser level.
③ By altering the relative population of $^4T_2$ and ^2E, the overall lifetime of the population inversion is altered.
④ At high inversion levels, as for example when Q-switching the laser may be inverted with respect to the $^2E - {}^4A_2$, 3 level laser scheme. Since the emission cross section is larger for the no-phonon transition it may dominate (and suppress) the phonon-terminated $^4T_2 - {}^4A_2$ transition.

A detailed discussion of the Alexandrite laser is given by Walling et al. [12] and Shand et al [13] with details of laser performance appearing in a number of papers [14-18] These include cw performance [15], Q-switched performance [16], mode locked performance [17] and high temperature performance [18]. Wide tunability, 726-502 nm has been demonstrated and high power operation (0.5J in 20 nsec pulses.) A particularly attractive feature of Alexandrite is that efficient pumping is possible with incoherent light sources (flash lamps) and so tunability is achieved directly without the need for pumping by another laser. However a detailed assessment of Alexandrite's performance cannot yet be made on the basis of the work published so far. The ultimate success of a solid state laser can depend on a number of features

other than just the spectroscopy and the level dynamics. For example important questions on optical quality, thermal distortion, damage threshold, etc, need to be thoroughly investigated.

The renewed interest in Cr^{3+} based laser materials has led to a number of potentially interesting candidates. Again it is too early to make a definitive assessment but the new materials show many interesting features. For example emerald ($Be_3Al_2(SiO_3)_6 : Cr^{3+}$) [19-20], offers wider tunability (700-850 nm) than Alexandrite and a larger emission cross section (up to 4 times larger). However the optical quality is not yet good enough. Other crystal hosts for Cr^{3+} which are under investigation include garnets [21-26] and most recently cw room temperature operation of Cr^{3+} in a fluoride host, $KZnF_3$ has been obtained, with tunability from 785-865 nm [27]. With the recent report of widely tunable operation of $Ti^{3+} : Al_2O_3$ (660-986 nm), [28] the prospects for tunable solid state lasers look very promising indeed,

6 References

1. L.F. Johnson, R.E. Dietz and H.J. Guggenheim, Phys. Rev. Lett. 11, (1963) 318-320
2. L.F. Johnson, R.E. Dietz and H.J. Guggenheim, Appl. Phys. Lett 5, (1964) 21-22
3. L.F. Johnson, H.J. Guggenheim and R.A. Thomas, Phys. Rev. 149 (1966) 179-185
4. L.F. Johnson & H.J. Guggenheim J. Appl. Phys. 38 (1967) 4837-4839
5. D.E. McCumber Phys. Rev. 134, 1964 A299-A306
6. P.F. Moulton, A. Moradian and T.B. Reed, Opt. Lett., 3 (1978) 164-166
7. P.F. Moulton and A. Mooradian, Appl. Phys. Lett 35 (1979) 838-840
8. B.C. Johnson P.F. Moulton and A. Mooradian, Optics Lett. 10 (1984) 116-118
9. P.F Moulton, IEEE J of Quantum Electron. QE-18 (1982) 1185-1189
10. W. Künzel, W. Knierim and U. Dürr, Optics Comm. 36 (1981) 383-386
11. L.F. Johnson, H.J. Guggenheim, D. Bahnk, and A.M. Johnson, Optics Letts. 8, (1983) 371-373

T. C. Peterson, H. P. Jenssen, R. C. Morris and E. W. O'Dell, IEEE. J. of Quantum Electron. QE-16, (1980) 1302 - 1314

13 M. L. Shand, J. C. Walling, H. P. Jenssen, IEEE. J. of Quantum Electron. QE-18 167-169

14 J. C. Walling, H. P. Jenssen, R. C. Morris, E. W. O'Dell and O. G. Peterson; Optics Letts 4 (1979) 182-183

15 S. T Lai and M. L. Shand, J. Appl. Phys. 54 (1983) 5642-5644

16 J. C. Walling and O. G. Peterson, IEEE. J. of Quantum Electron. QE-16 (1980) 119 - 121

17 V. N. Lisitsyn et al. Sov. J. Quantum Electron. 12 (1982) 368 - 370

18 S. Guch and C. E. Jones, Optics letters 7, (1982) 608-610

19 M. L. Shand and J. C Walling, IEEE J. of Quantum Electron., QE-18 (1982) 1829 - 1830

20 J. Buchert, A. Katz and R. R Alfano, IEEE. J. of Quantum Electron. QE-19 (1983) 1477 - 1478

21 H. P. Christensen and H. P. Jenssen, IEEE. J of Quantum Electron. QE-18, (1982), 1197 - 1201

22 P. T. Kenyon, L. Andrews, B. McCollum, and A. Kempicki IEEE. J of Quantum Electron. QE-18, (1982) 1189 - 1197

23 G. Huber, B. Struve, Chromium doped crystals for tunable lasers, Lasers '82, NEW ORLEANS

G. Huber, J. Drube and B. Struve, Recent developments in tunable Cr doped garnet lasers; Lasers '83, San Francisco.

5 G. Huber and K. Petermann, laser action in Cr doped garnets and tungstates, 1st Annual conference on tunable solid state lasers, LaJolla, USA 1984

6 J. Drube, B. Struve and G. Huber, Optics Comm. 50, (1984) 45-48

U. Brauch and U Dürr, Optics Letts, 9 (1984) 441-442

P. F. Moulton, New Developments in Solid State Lasers, Laser Focus, May 1983, 83 - 88

Difference frequency generation and parametric generation.

The basic principles and details of the analytical treatment are given in [1-3].

We consider a medium having a nonlinear response in the sense that the polarisation induced by an applied field depends on the square of the field.

$$P = \chi^{(1)}E + \chi^{(2)}EE + \ldots$$

The second term is nonzero only in non-centrosymmetric media so the phenomenon is restricted to certain crystal classes.

The presence of the $\chi^{(2)}EE$ term implies that if waves of frequency ω_2, ω_3 are input to the medium, a polarisation will be generated at frequency $\omega_1 = \omega_3 - \omega_2$ (also $2\omega_3, 2\omega_2, \omega_3+\omega_2$) and this will radiate a wave of frequency $\omega_3 - \omega_2$. This is difference frequency generation.

In practice for efficient generation a number of requirements must be met.

(1) The wave vectors must satisfy the phase-matching condition $\underline{k}_1 = \underline{k}_3 - \underline{k}_2$, which for collinear waves is simply $k_1 = k_3 - k_2$ or $n_1\omega_1 = n_3\omega_3 - n_2\omega_2$ where the n are refractive indices.

In general dispersion will preclude the achievement of phase-matching, however in crystals with sufficient birefringence, the birefringence can be used to offset dispersion and the phase mismatch Δk ($\equiv k_3 - k_2 - k_1$) can be made zero.

N2.2 (1)

(2) The medium must have a large nonlinearity $\chi^{(2)}$. Usually the nonlinearity is expressed in terms of a quantity d, proportional to $\chi^{(2)}$ (see [1]-[3]). A figure of merit for the nonlinearity of the medium is $\frac{d^2}{n_1 n_2 n_3}$ 2 (2)

(3) The medium must be transparent for $\omega_1, \omega_2, \omega_3$

(4) The crystal must be of good optical quality

(5) Typically crystal dimensions (in the direction of propagation) must be of the order of centimetres.

(6) The crystal must be able to withstand high intensity laser beams, e.g. pulsed (nanosecond) intensities of $\sim 100\,MW/cm^2$, without damage

Relatively few crystals have been found to satisfy these requirements to the extent that practical devices can be developed.

Some successful examples are

	d^2/n^3 (relative)	Transmission
$LiNbO_3$	~4	0.35 – 4.5 μm
$LiIO_3$	~2	0.31 – 5.5 μm
Ag_3AsS_3	~8	0.6 – 13 μm
$AgGaS_2$	~11	0.6 – 13 μm
KDP	~0.08	0.22 – 1.1 μm

(1)

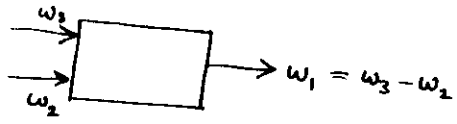

'Difference frequency generation' of ω_1. Either ω_3 or ω_2 can be tunable, hence producing tunability of ω_1.

Note that in photon terms we have

$$\hbar\omega_3 - \hbar\omega_2 = \hbar\omega_1$$

Thus photons of the highest frequency ω_3 are annihilated and photons of frequency ω_1 and ω_2 are generated. So frequency ω_2 is amplified.

(2) Optical parametric amplification (OPA)

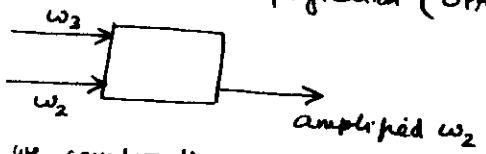

Here we consider the situation where a large amplification of ω_2 is achieved (ω_3 is a powerful pump). This can be used either as a means of amplifying a weak signal or as a means of generating a significant power at the idler frequency $\omega_1 = \omega_3 - \omega_2$. The output power at the idler is (for large gain) equal to $\frac{\omega_1}{\omega_2}$ times the output signal power.

Typically ω_3 can be a powerful fixed frequency laser and ω_2 a weak tunable laser.

(3) Superfluorescent parametric emission.

Here the gain is so high that ω_1, ω_2 can grow to significant levels starting from noise.

The particular pair of frequencies ω_1, ω_2 (which must always satisfy $\omega_3 = \omega_1 + \omega_2$) that dominate in the output are those for which the phase-matching condition is satisfied, i.e

$$k_3 = k_1 + k_2.$$

So one can tune the output frequency by tilting the crystal. Note that this scheme gives a tunable output despite the input being a fixed frequency.

(4) Parametric oscillation.

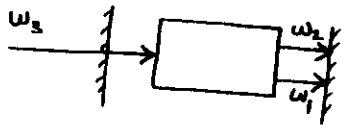

Again ω_1, ω_2 grow from noise, assisted by feedback from the mirrors. Tuning of ω_1, ω_2 is achieved by changing the phase-matching.

The optical parametric oscillator (OPO) can either have mirrors providing feedback for both ω_1 and ω_2 (doubly-resonant oscillator) or for just one of ω_1 and ω_2 (singly-resonant oscillator)

A general analysis which encompasses difference frequency generation, optical parametric amplification, superfluorescent parametric emission and parametric oscillation is found in ref [1]. The results are quoted here

Assuming all the waves to be propagating in the z-direction,

with fields given by

$$E_1(z,t) = \tfrac{1}{2}\left[E_1(z)\exp i(k_1 z - \omega_1 t) + \text{c.c.}\right]$$

$$E_2(z,t) = \tfrac{1}{2}\left[E_2(z)\exp i(k_2 z - \omega_2 t) + \text{cc.}\right]$$

and assuming no pump depletion $\left(dE_3/dz = 0\right)$ and no attenuation of waves 1 and 2, the following differential equations are obtained [1]

$$\frac{dE_1(z)}{dz} = i\left(\frac{\omega_1 d}{n_1 c}\right) E_3 E_2^* \exp(i\Delta k z) \qquad (1)$$

$$\frac{dE_2(z)}{dz} = i\left(\frac{\omega_2 d}{n_2 c}\right) E_3 E_1^* \exp(i\Delta k z) \qquad (2)$$

Solving these equations for E_1, E_2 it is found that the fields $E_1(\ell)$, $E_2(\ell)$ after propagating through a length ℓ of nonlinear medium (of refractive indices n_1, n_2, n_3 and effective nonlinear coefficient d) are

$$E_1(\ell) = E_1(0)\, e^{i\Delta k\ell/2}\left[\cosh g\ell - i\frac{\Delta k}{2g}\sinh g\ell\right] + i\omega_1 d\frac{E_3 E_2^*(0)}{n_1 c} e^{i\Delta k\ell/2}\sinh g\ell \qquad (3)$$

$$E_2(\ell) = E_2(0)\, e^{i\Delta k\ell/2}\left[\cosh g\ell - i\frac{\Delta k}{2g}\sinh g\ell\right] + i\frac{\omega_2 d E_3 E_1^*(0)}{n_2 c} e^{i\Delta k\ell/2}\sinh g\ell \qquad (4)$$

where $g = \left[\underbrace{\frac{\omega_1\omega_2 d^2|E_3|^2}{n_1 n_2 c^2}}_{=\Gamma^2} - \left(\frac{\Delta k}{2}\right)^2\right]^{1/2}$ (5)

With input $E_2(0)$, but no input E_1 (i.e. $E_1(0) = 0$), defining the gain $G_2(\ell)$ of the wave 2 as the fractional increase in intensity, i.e.

$$G_2(\ell) = \left|\frac{E_2(\ell)}{E_2(0)}\right|^2 - 1 \qquad (6)$$

we obtain

$$G_2(\ell) = \frac{\Gamma^2\ell^2 \sinh^2(g\ell)}{(g\ell)^2} \qquad (7)$$

For small gain $\Gamma\ell$ and for $(\Delta k\ell/2)^2 \gg \Gamma^2\ell^2$ this gives $G_2(\ell) = \Gamma^2\ell^2 \operatorname{sinc}^2\left(\frac{\Delta k\ell}{2}\right)$.

The generated wave 1 therefore has an intensity

$$I_1(\ell) = I_2(0)\, G_2(\ell)\, \omega_1/\omega_2$$

$$= I_2(0)\frac{\omega_1^2}{n_1 n_2 c^2} d^2 |E_3|^2 \ell^2 \operatorname{sinc}^2\left(\frac{\Delta k\ell}{2}\right)$$

$$= \frac{2\omega_1^2 d^2 I_2(0)}{\epsilon_0 c^3 n_1 n_2 n_3} I_3 \ell^2 \operatorname{sinc}^2\left(\frac{\Delta k\ell}{2}\right) \qquad (8)$$

This equation gives the generated intensity $I_1(\ell)$ for input intensities $I_2(0)$, I_3.

Note; the figure of merit for the nonlinear medium is $d^2/n_1 n_2 n_3$

; it is desirable to work with high input intensities I_2, I_3

; efficient generation is in general more difficult for longer wavelengths (smaller ω_1)

; a long crystal is desirable provided $\Delta k\ell/2$ remains small

$$G_2(l) = \tfrac{1}{4} \exp \Gamma l$$

$$= \tfrac{1}{4} \exp \left\{ \frac{8 \omega_3 \omega_2 d^2 I_3 l^2}{\epsilon_0 n_1 n_2 n_3 c^3} \right\}^{1/2}$$

thus showing an exponential growth with distance through the medium. Note that the exponent varies as $I_3^{1/2}$ unlike the case of Raman scattering where the exponent varies as I_p.

Some examples of experimental results are listed.

1/ $LiNbO_3$ optical parametric oscillator pumped by 1.06μm, refs. [4, 5]. A tuning range of ~1.4 – 4.5 μm is achieved, with energy conversion efficiency ranging from 50% down to a few %.

2/ Optical parametric amplification in $LiNbO_3$ [6]
High gain (×80) demonstrated for a 1.9 μm signal using a 1.06 μm pump.
High efficiency also demonstrated with ~15% conversion of pump to signal.

3 Difference frequency generation: ~~three examples~~; a low power (10 μW) source of single frequency radiation, tunable from 0.94 to 1.40 μm, obtained by mixing a 1w dye laser and 1w NdYAG laser output in $LiNbO_3$ [7]; a widely tunable source, 5.5 – 18.3 μm obtained by mixing two dye laser outputs in $AgGaS_2$ [8]; also using $AgGaS_2$, Kato [9] achieved tuning from 5 – 11 μm with peak outputs as high as 180 kW and an average power up to 14 mW

[illegible] emission. Several examples in recent years, using picosecond pump pulses, giving very widely tunable picosecond pulses; [10–15]. For example [13], 1.2 – 8 μm in proustite (Ag_3AsS_3), and 1.2 – 10 μm in $AgGaS_2$ [15].

References

1. R.L. Byer, Chapter 2 'Parametric Oscillators and Nonlinear Materials' in Nonlinear Optics, Proc. of 16th Scottish Universities Summer School in Physics 1977. Eds. P.G. Harper and B.S. Wherrett, Academic Press 1977.
2. Y.R. Shen, The Principles of Nonlinear Optics, Wiley-Interscience 1984.
3. O. Svelto, Principles of Lasers (2nd Edn), Plenum Press, (1982)
4. R.L. Herbst, R.N. Fleming and R.L. Byer, Appl. Phys. Letts. 25 (1974), 520-522
5. S.J. Brosnan and R.L. Byer, IEEE J. of Quantum Electron. QE-15 (1979) 415-431
6. R.A. Baumgartner and R.L. Byer, IEEE J. of Quantum Electron. QE-15 (1979) 432-444
7. N.P. Barnes et al., Lasers '82, New Orleans LA, December 13-17, 1982
8. R.J. Seymour and F. Zernike, Appl. Phys Letts. 29 (1976) 705-707
9. K. Kato, IEEE J of Quantum Electronics QE-20, (1984) 698-699
10. A. Laubereau, L. Greiter and W. Kaiser, Appl. Phys. Letts, 25 (1974) 87-89
11. A. Seilmeier, K. Spanner, A. Laubereau and W. Kaiser Optics Commun. 24 (1978) 237-242
12. A. Seilmeier and W. Kaiser, Appl. Phys. 23 (1980), 113-119
13. T. Elsaesser, A. Seilmeier and W. Kaiser, Optics Commun. 44 (1983) 293-296
14. F. Wondrazek, A. Seilmeier and W. Kaiser, Appl. Phys B, 32, (1983), 39-42.
15. T. Elsaesser, A. Seilmeier and W. Kaiser, Appl. Phys. Letts. 44 (1984) 383-385.

... [1-8] provide a useful range of review articles/book chapters.

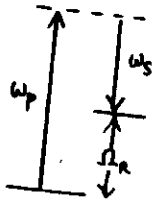

$$\hbar\omega_s = \hbar\omega_p - \hbar\Omega_R$$

$$\omega_s = \omega_p - \Omega_R$$

A pump wave, of frequency ω_p is down-converted in frequency to a 'Stokes' wave of frequency ω_s. Hence pump tunability can be transferred from the visible region to the infrared.

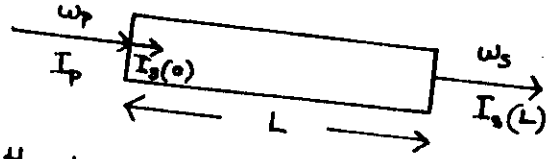

In the steady-state, Stokes intensity $I_s(L)$ leaving the Raman medium is given by

$$I_s(L) = I_s(0)\exp(g_R I_p L) \qquad (1)$$

$I_s(0)$: noise from spontaneous Raman scattering, $\sim h\nu\Delta\nu$

require $\sim \exp(30)$ to reach 'threshold'

The Raman gain coefficient g_R depends only on the parameters of the medium.

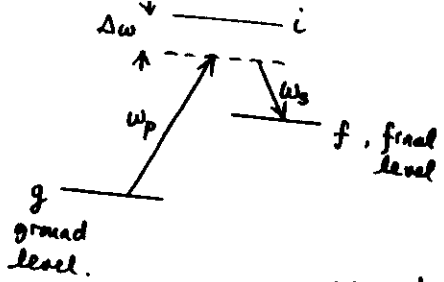

$\Delta\omega$ is the detuning of the pump frequency from the intermediate level i

$$g_R \propto \frac{N\omega_s}{\Gamma}\left|\sum_i\left(\frac{\mu_{gi}\mu_{if}}{\omega_{ig}-\omega_p} + \frac{\mu_{gi}\mu_{if}}{\omega_{ig}+\omega_s}\right)\right|^2 \qquad (2)$$

where N is the number density of scatterers in the initial level (g), Γ is the linewidth of the Raman transition $g \to f$, and the μ are electric dipole matrix elements (see ref [6] for details)

If only one intermediate level i is dominant then

$$g_R \propto \frac{N f_{gi} f_{if} \omega_s}{\Gamma(\Delta\omega)^2} \qquad (3)$$

This expression displays the most important dependences, on $(\Delta\omega)^{-2}$, on ω_s, on Γ^{-1}, on N and on the oscillator strengths f.

The full expression is

$$g_{R\,(peak)} = \frac{N e^4 \nu_s f_{gi} f_{if}}{32\pi^3\epsilon_0^2 hc^2 m_e^2 \nu_{ig}\nu_{if}(\nu_{gf}-\nu_p)\Delta\nu_R} \qquad (4)$$

$\Delta\nu_R$ is the Full Width Half Maximum, and all frequencies, including $\Delta\nu_R$ are in Hz

If oscillator strengths are not known, or the summation over intermediate states cannot be calculated, then one must use experimental data on the differential Raman cross section, $d\sigma_R/d\Omega$

$$g_R = \frac{2c^2 N}{\pi h n_s^2 \nu_s^3 \Delta\nu_R} \cdot \left(\frac{d\sigma_R}{d\Omega}\right) \qquad (5)$$

($\frac{d\sigma_R}{d\Omega}$ is defined in terms of incident and scattered intensities, rather than photon numbers. Tabulated values of $d\sigma_R/d\Omega$, eg ref. [8] are usually in terms of intensities)

Using expression (5) or (4) for g_R, and the threshold condition $g_R I_p L \simeq 30$, one can calculate the Raman threshold power.

Example Stimulated Raman Scattering in H_2 gas, on the $Q_{01}(1)$ transition ($\Omega_R \equiv 4155.2\ cm^{-1}$); from (5) it can be shown that $g_R = \frac{2.4 \times 10^{-3}}{\lambda_s(\mu m)}$ cm/Mw

If $\lambda_s = 0.8\mu m$ (i.e. $\lambda_p = 0.6\mu m$), then $g_R = 3\times10^{-3}$ cm/Mw

Since threshold requires $g_R I_p L \simeq 30$, then $I_p L = 10^4$ Mw/cm

Assume a TEM_{00} pump, with confocal focussing in the Raman cell, i.e. $\frac{2\pi w_0^2}{\lambda_p} = L$

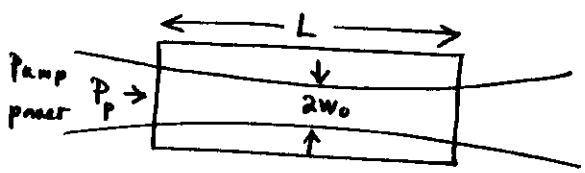

Then (roughly), $I_p L = \frac{P_p}{\pi w_0^2} L = \frac{P_p}{\pi w_0^2} \cdot \frac{2\pi w_0^2}{\lambda}$

$= 2P_p/\lambda_p$

So $2P_p/\lambda_p = 10^4$ Mw/cm

$\therefore P_p = 0.3$ Mw

Thus a typical threshold power for SRS in H_2 gas is $\sim$ 1 Mw. Note that the calculation assumed a diffraction-limited beam. If the beam divergence is m times greater than diffraction limited, then the threshold is m times greater.

The model calculation above assumed steady-state conditions. We now consider transient Raman scattering.

The Raman linewidth $\Delta\nu_R$ and the dephasing time T_2 of the Raman excitation (e.g. the molecular vibration in the case of H_2) are related by

$$T_2 = \frac{1}{\pi\Delta\nu_R} \qquad (6)$$

For steady-state conditions to apply (and hence equation

to apply) the pump pulse duration must be greater than T_2. In practice the condition for steady state is more like $t_p \gtrsim 20T_2$. When the inequality is reversed the Raman process is transient, and for $t_p \lesssim T_2$ the threshold is characterised by a pump energy rather than a power. A detailed analysis of transient Raman scattering is given in [9]. A useful result which applies when $t_p < T_2$ is that, assuming a square shaped pump pulse, the pump intensity to reach threshold is given by

$$g_R I_p L \simeq 100\left(\frac{T_2}{t_p}\right) \qquad (7)$$

which can be rewritten as

$$g_R E_p L \simeq 100\, T_2 \qquad (8)$$

where $E_p = I_p t_p$ is the pump energy to reach threshold.

Also note that since $g_R \propto \Gamma^{-1} \propto T_2$ (equation (3)) then E_p is independent of T_2. Thus for transient SRS the threshold energy is independent of the Raman linewidth, whereas for steady state SRS the threshold power is proportional to linewidth.

We now consider three Raman media, of very different kinds, all three of which have demonstrated useful capability for generating tunable infrared radiation.

They are (i) hydrogen gas, (ii) caesium vapour and (iii) glass, in the form of an optical fibre waveguide.

Useful references on the performance of these media are [10-12] for H_2, [13-15, 6] for Cs vapour, [16-20] for glass fibre waveguides.

Significant features of these media, and their consequences are now briefly mentioned.

Hydrogen (i) Good transparency from UV (~150nm) to longer wavelengths, right through the infrared.

(ii) Narrow Raman transition linewidth, $\Delta\nu_R \simeq 40p$ MHz where the pressure p is in atmospheres. So a 20nsec pump pulse produces steady state conditions for $p \gtrsim 20$ atmospheres.

(iii) Raman shift 4155 cm^{-1}. Hence if a dye laser is used as pump, as many as three sequential Raman shifts are needed to produce near infrared radiation [10].

(iv) A gain $g_R = \dfrac{2.4\times10^{-3}\ cm/MW}{\lambda_s(\mu m)}$ implies the need for megawatt pump power levels usually. A useful reduction of threshold can be achieved by confining the gas to a hollow capillary waveguide [10], with an order of magnitude reduction being typical [12,21].

(v) An example of performance achieved with H_2 is reported by Hartig and Schmidt [10].
The dye laser pump tuned from 550-720nm; Laser pulse duration 10nsec and pulse energy ~ 35mJ at 565nm and ~20mJ at 690nm.
This gave a Stokes tuning range of 0.7 - 7.0 μm (1st, 2nd and 3rd Stokes)
18mJ (1.8kW) at 690nm gave 80μJ (~15kW) at 5.2μm (3rd Stokes); Hence 1/2% energy conversion, 1% power conversion, 3 1/2 % photon conversion.

Caesium vapour.

(i) The Raman shift is very large compared to H_2 since the transition is an electronic transition (rather than vibrational, as in H_2). The shift is ~ 14500 cm^{-1} for the 6s → 5d transition, ~18,500 cm^{-1} for the 6s → 7s transition. So a single Raman shift is sufficient to convert a dye laser pump to infrared wavelengths.

(ii) Number densities are much lower than in H_2. Typical vapour pressures are 10 - 100 Torr. Even at these vapour pressures there is a significant population of Cs_2 dimers which have absorptions in the visible region. [6]

(iii) Since the detuning, $\Delta\omega$, of the pump frequency from the intermediate level can be made small (say a few hundred cm^{-1}) a large resonant enhancement of the Raman gain can be achieved. Threshold powers of a few kW up to ~1MW are typical.

(iv) The transition linewidth is narrow $\lesssim 1 cm^{-1}$, hence narrow linewidth (~ 0.5 cm^{-1}) infrared radiation can be generated

(v) Wide tunability has been achieved; 1.6 - 3.2 μm [13], 2.9 - 11.1 μm [14], 2.5 - 4.75 μm, 5.7 - 8.6 μm, 11.7 - 15 μm [22]

Glass fibre waveguide.

(i) The Raman gain coefficient in fused silica is small; for a 1.06 μm pump, $g_R = 0.9 \times 10^{-9}$ cm/W [23] This is around two orders of magnitude smaller than g_R for H_2 gas.

(ii) The Raman shift is small, ~ 400 cm^{-1}, thus necessitating several Raman shifts to produce infrared wavelengths.

(iii) The Raman linewidth is large (~300 cm^{-1} FWHM) [23]. This accounts for the small g_R (see equation (5)). An advantage of the broad linewidth is that it provides tunability of the Stokes radiation.

(iv) Fused silica has good transparency (even over hundreds of metres length) to wavelengths as long as ~ 2 μm.

(v) By using an optical fibre waveguide one can achieve a high intensity for a low pump power and maintain this high intensity over very great lengths. Thus $g_R I_p L$ can be large enough to reach threshold with pump powers of a few tens of watts.
The use of a fibre waveguide, with very long interaction lengths involved, introduces additional features that need to be considered. For example the dispersion of the waveguide has

significant effects. Around 1.1 μm, a dispersion of around 30 ps/nm km has been measured [16]. By operating the Raman oscillator as a synchronously pumped oscillator the Stokes wavelength can be tuned by fine tuning the resonator length, thus choosing the Stokes wavelength which achieves synchronism [16]

(VI) Very wide tuning ranges have been achieved, 0.6 – 1.8 μm [17] and 1.1 – 1.6 μm [19], by pumping hard enough to allow multiple Stokes shifts to occur.

(VII) By diffusing H_2 or D_2 gas into fused silica waveguides, one gets a high density of molecules (equivalent to the density reached in ~ 10 atmospheres of gas.) Stimulated Raman scattering from the gas molecules has been observed and efficient conversion from 1.06 μm to 1.56 μm has been achieved with D_2 in glass [24,25]. This needs only one Stokes shift ($2988\ cm^{-1}$). This scheme offers the combined advantage of the molecule (large shift, narrow linewidth) and the waveguide (low pump power requirement.)

References

1. N. Bloembergen, Am. J. of Phys. 35 (1967), 989-1008
2. W. Kaiser and M. Maier: in Laser Handbook ed. by F.T. Arecchi and E.O. Schultz-Dubois (North Holland, Amsterdam 1972), Vol 2 p 1077-1150
3. M. Maier, Appl. Phys. 11 (1976), 209-231
4. A.Z. Grasiuk and I.G. Zubarev, Appl. Phys. 17 (1978), 211-232
5. A. Penzkofer, A. Laubereau and W. Kaiser, Prog. Quant. Electr. 6, 55-140
6. D.C. Hanna, M.A. Yuratich and D. Cotter: Nonlinear Optics of Free Atoms and Molecules, Vol 17, Springer Series in Optical Sciences, Spring-Verlag 1979
7. Y.R. Shen. The Principles of Nonlinear Optics, Wiley-Interscience 1984
8. H.W. Schröter and H.W. Klöckner, in vol II, Topics in Current Physics, ed. A. Weber, Springer-Verlag 1979
9. R.L. Carman, F. Shimizu, C.S. Wang and N. Bloembergen, Phys. Rev. A, 2, (1970) 60-72
10. W. Hartig and W. Schmidt, Appl. Phys. 18 (1979) 235-241
11. M. Bierry, R. Frey and F. Prudine, Rev. Sci Instrum. 48 (1977) 733-737
12. A.J. Berry, D.C. Hanna and D.B. Heath, Optics Commun. 43 (1982) 229-232

(References continued.)

13 R. Wyatt and D. Cotter, Appl. Phys. 21 (1980) 199-204

14 A.L. Harris, J.K. Brown, M. Berg and C.B. Harris, Optics Letts 9 (1984) 47-49

15 M. Berg, A.L. Harris, J.K. Brown and C.B. Harris, Optics Letts 9 (1984) 50-52

16 Chialou Lin, R.H. Stolen and L.G. Cohen, Appl. Phys. Letts, 31 (1977) 97-99

17 K. Kitayama, Y Kato, S. Seikai and M. Tateda, Appl. Optics 20 (1981) 2428-2432

18 C. Lin, L.G. Cohen, R.H. Stolen, G.W. Tasker and W.G. French, Optics Comm. 20 (1977) 426-428

19 L.G. Cohen and C. Lin, IEEE J. Quant. Electron., QE-14 (1978) 855-859

20 G. Pei-juan, N. Cao-jiang, Y. Tian-long and S. Hai-zheng, Appl. Phys. 24 (1981) 303-306

21 A.J. Berry and D.C. Hanna, Optics Commun. 45 (1983) 357-360

22 D. Cotter, D.C Hanna and R. Wyatt, Optics Commun. 16 (1976) 256-258

23 R.H. Stolen and E. Ippen, Appl. Phys. Lett. 22, (1973) 276-278

(References continued)

24 J. Stone, A.R. Chraplyvy and C.A. Burrus, Optics Letters, 8 (1983) 415-417

25 A.R. Chraplyvy and J. Stone, Optics Letters, 9 (1984) 241-242